Applied Surface Science 187 (2002) 319–325

applied surface science

www.elsevier.com/locate/apsusc

Structure and morphology of concave-shaped surfaces on 6H–SiC(0 0 0 1) after H_2 etching

Frédéric Dulot[a,1], Louay Mansour[a], André Leycuras[b], Wulf Wulfhekel[a,2], Dirk Sander[a,2], François Arnaud d'Avitaya[a], Margrit Hanbücken[a,*]

[a]*CRMC2-CNRS, Campus de Luminy, Case 913, F-13288 Marseille, France*
[b]*CRHEA-CNRS, Rue Bernard Gregory, Sophia-Antipolis, 06560 Valbonne, France*

Received 1 November 2001; accepted 9 December 2001

Abstract

Concave-shaped surfaces have been prepared on 6H–SiC(0 0 0 1) substrates by exposing troughs, prepared by dimple grinding of flat SiC surfaces, to H_2 at high temperature. The morphological changes occurring under this H_2 etching were studied using scanning electron microscopy (SEM), atomic force microscopy (AFM) and ultrahigh vacuum scanning tunnelling microscopy (UHV-STM). Already after heating in H_2 at 1600 °C for 20 min, morphological changes are observed and heating in H_2 at 1700 °C for 15 min leads to the formation of alternating large and small terraces, separated by straight steps of 0.75 nm height on the flat parts of the substrate. A model is proposed which ascribes this bimodal terrace size distribution to the atomic structure of the SiC steps and to H diffusion on the terraces. For the same etching conditions less significant morphological variations were detected on the curved areas of the surface, where dimple grinding had been performed. The beginning of a considerable structural reorganisation of the concave-shaped surfaces was detected only when the etching temperature was increased to 1700 °C and the etching time to 1 h. Then, terrace steps with preferential edge orientation along the family of $[1\,1\,\bar{2}\,0]$ directions are formed in the concave-shaped areas, as observed by SEM. © 2002 Elsevier Science B.V. All rights reserved.

Keywords: Concave-shaped surface; 6H–SiC; Scanning electron microscopy; Atomic force microscopy; Ultrahigh vacuum scanning tunnelling microscopy

1. Introduction

Silicon carbide has become a very important semiconductor material because of its interesting electronic and structural properties. Compared to silicon, germanium or compound semiconductors, SiC is an excellent candidate for potential devices functioning at higher temperatures and high frequencies [1]. The crystallography of SiC is complex. It crystallises as a polytype with over 200 different variations and the stacking sequence of the hexagonal bilayers defines the different polytypes. In epitaxial growth experiments, the polytype 6H–SiC(0 0 0 1) is increasingly used as a substrate [2]. For the homoepitaxial growth of SiC films, vicinal, the so-called off-axis 6H–SiC substrates are used [3–5]. The SiC surface structure, surface reconstruction and the terrace and step distribution on these vicinal surfaces influence the growth

---

[*] Corresponding author. Fax: +33-491-41-8916.
E-mail address: margrit.hanbucken@crmc2.univ-mrs.fr (M. Hanbücken).

[1] Present address: Faculté des Sciences et Technologies, Laboratoire de Physique et de Spectroscopie Electronique, 4 Rue des Frères Lumière, F-68093 Mulhouse, France.

[2] On leave of abscence from: Max-Planck-Institut für Mikrostrukturphysik, Halle, Germany.

0169-4332/02/$ – see front matter
PII: S0169-4332(01)01048-0

conditions and the quality of the films. A detailed knowledge of vicinal surfaces of SiC is therefore of importance. In prior work on silicon, we have been able to develop a universal sample for the study of vicinal surfaces, by transforming concave-shaped surfaces into an extended set of vicinals by thermal treatment [6]. In the case of Si(1 1 1), these curved surfaces split up into terraces and steps whose morphology and size reflect the threefold symmetry of the crystal. In extension of our previous work on Si, our objective is to investigate the influence of a locally varying misorientation of a SiC sample on the morphology changes induced by H_2 etching. In previous work it has been shown that on flat, on-axis SiC surfaces, polishing-induced damage can be eliminated by H_2 etching [7], giving rise to the reorganisation of the surfaces into uniformly spaced, flat terraces, separated by steps [8,9]. Morphology changes on off-axis, vicinal 6H–SiC(0 0 0 1) substrates under H_2 etching have been studied by Xie et al. [10]. These authors conclude that the observed surface morphology is essentially defined by the initial misorientation of the vicinal SiC surface. The H_2 etch rate was found to be 30–40% smaller on misoriented surfaces as compared to on-axis, flat SiC surfaces [10]. Here, we investigate the interplay between H_2 etching temperatures and etching times and the resulting morphology changes on SiC samples with locally varying misorientation, as prepared from concave-shaped surface.

2. Experimental

The samples (4 × 15 mm^2) were cut from an on-axis (nominally no misorientation), nitrogen-doped, n-type (resistivity 0.03–0.12 Ω cm) 6H–SiC(0 0 0 1) wafer, delivered by SiCrystal, Germany. A concave-shaped surface depression was created in the middle of the sample by a dimple grinder, using diamond paste with a grain size of 3 μm. Grinding was stopped when a depth of about 30 μm was obtained in the middle of the dimple. The diameter of the dimple was about 1.5 mm, as checked by scanning electron microscopy (SEM). Prior to hydrogen (H_2) etching, the samples were cleaned in methanol in an ultrasonic bath. H_2 etching was performed in a horizontal graphite hot-wall chemical vapour deposition (CVD) reactor [11] at an H_2 pressure of 13 mbar. Etching temperatures were varied between 1600 and 1750 °C and the etching time, i.e. the time of exposure of the sample at high temperature to H_2 were increased from 5 min to 1 h. At this high temperature, thermal decomposition of SiC has to be anticipated, leading to the so-called sublimation etch of SiC [7]. However, step heights of several multiples of three SiC bilayers have been reported for sublimation etch [7], whereas we observe step heights of three SiC bilayers, which indicates that H-etching is the predominant etch mode. The etched samples were subsequently characterised by atomic force microscopy (AFM) [12] and ultrahigh vacuum scanning tunnelling microscopy (UHV-STM) [13]. To follow the evolution of the etching process, AFM, STM and SEM images were taken on the flat parts and in the dimpled area of the sample after removal from the CVD reactor.

3. Results and discussion

An overview SEM image from the dimpled 6H–SiC sample is given in Fig. 1. The concave-shaped dimple

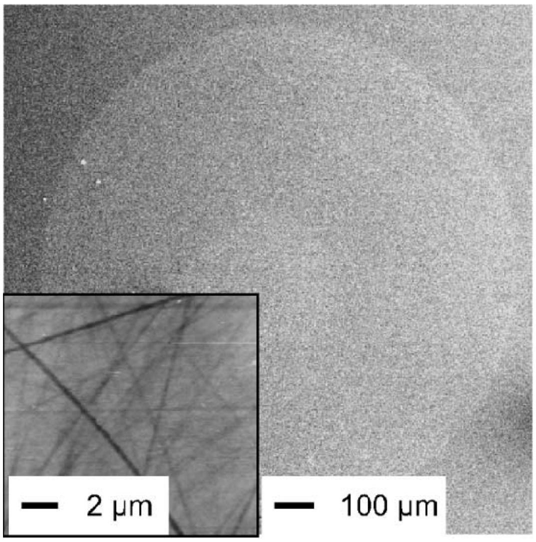

Fig. 1. SEM overview image of the 6H–SiC substrate showing the flat parts and the concave-shaped dimple, to be recognized as the brighter circular area in the middle. The inset shows an AFM image of the flat surface area before H_2 etching. The dark lines are due to scratches from the polishing process. The grey scale contrast between these lines and the neighbouring flat areas corresponds to 14 nm.

can be distinguished from the flat parts of the sample by the brighter grey tone seen in the dimpled area. The initial roughness of the flat parts of the sample, as-received from SiCrystal, is shown by the AFM image of the inset in Fig. 1. A large amount of scratches due to surface polishing is apparent. After AFM imaging, the sample has been etched for different time intervals and at different temperatures in H_2. Starting from 1600 °C for 15 min typical rearrangements of the 6H–SiC(0 0 0 1) surface into terraces and steps have been observed on the flat parts of the substrate. Fig. 2 shows an STM image of these rearrangements on the flat parts of the substrate. This image was taken after H_2 etching at 1700 °C for 15 min. Flat terraces separated by very straight steps along $\{\bar{1}2\bar{1}0\}$ were formed. In agreement with previous work, the H_2 etching has removed all scratches of the as-prepared sample, shown in the inset of Fig. 1. The STM image of Fig. 2 taken with a calibrated scanner of the scanning tunnelling microscope reveals uniform step heights of 0.75 nm height corresponding to three double layers of SiC. Interestingly, the observed terraces show regularly alternating large and small width. Additional etching did not change this structure. This bimodal terrace width distribution can be ascribed to the layer structure of 6H–SiC. Along the *c*-axis of the crystal, the hexagonal SiC double layers are arranged in two groups of three double layers, each. Within each group, the stacking is hexagonal, but from one group to the other, the lattice is rotated by 60°. As a consequence, the closed-packed step edges on 6H–SiC change their nature going from one group to the other. The character of steps running along low index directions alternates between S_N and S_D step edges [14] (step nomenclature according to Pechman et al. [15]), i.e. the bonding at the step edge itself shows either one (S_N) or two (S_D) dangling bonds. It was expected that these different atomic structures of the steps lead to different H_2 etch rates [14]. In the observed step arrangement with step bunches of only three double layers high, the nature of the bonding is alternated and step edges on adjacent terraces are terminated differently such that one of them is etched faster. This causes an imbalance in the terrace width.

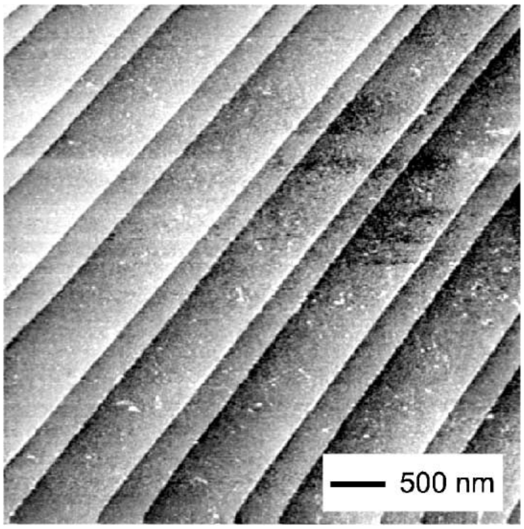

Fig. 2. STM image from a flat part of the SiC crystal after H_2 etching for 15 min at 1700 °C. $V_{\mathrm{gap}} = -3.28$ V, $I_t = 1$ nA. Flat terraces separated by straight steps of 0.75 nm height are obtained. The terrace width shows a bimodal distribution, it varies from wide to narrow for adjacent terraces.

However, a generally faster etching of one type of a step edge should lead to the elimination of terraces by formation of larger step bunches of at least the full unit cell height. This is not observed in our images, indicating that there is a compensating mechanism. If the relevant reaction step of the etching is hydrogen adsorption on the step edges themselves, the different etch rates persist no matter how wide the terraces are and the slowly etched type of step edges is caught up by the fast one. However, if the relevant step is the adsorption of hydrogen on the flat terraces followed by diffusion towards the lower step edge, the fast etching of one of the types of steps will be slowed down by the shrinking of the size of the hydrogen supplying terrace and a stable bimodal step configuration may be reached. Under equilibrium conditions, the width of the terraces is inversely proportional to the etching rate of the lower step edge indicating a ratio of etch rates of about 2:5 at the different step edges. Which of the two types of step edges is etched faster than the other is however not possible to tell from our STM data, since the resolution was not sufficient to resolve the atomic structure of the step edges. Similar bimodal terrace width distributions have been found on terraces winding around a micropipe defect, as presented in a recent paper by Madar et al. [16].

The above-mentioned etching conditions produced very different and distinct morphological changes on the concave-shaped parts of the sample, as shown in the AFM images of Fig. 3, which were taken in the dimple.

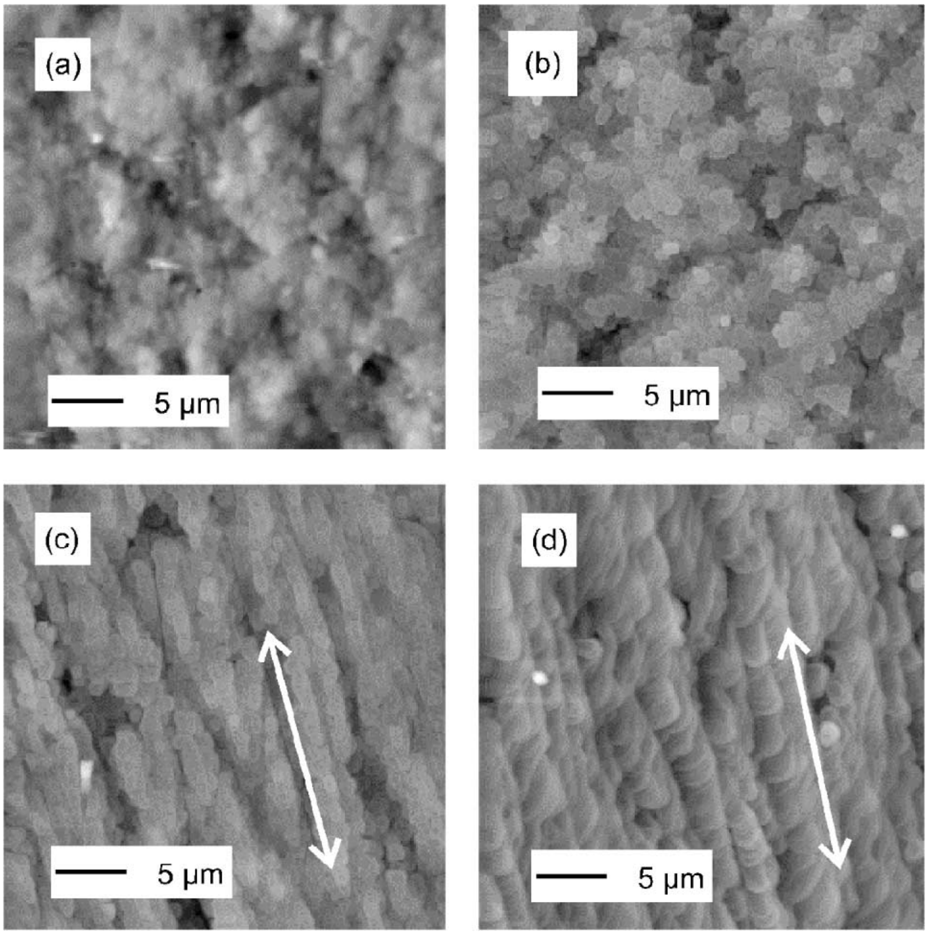

Fig. 3. AFM images obtained on the concave-shaped parts of the SiC: (a) surface after grinding (vertical range 642 nm); (b) after H_2 etching at 1600 °C for 5 min (vertical range 507 nm); (c) after additional H_2 etching at 1600 °C for 15 min (vertical range 476 nm); (d) after additional H_2 etching at 1700 °C for 15 min (vertical range 387 nm). The arrow indicates a preferential step edge orientation along a $[1\,1\,\bar{2}\,0]$-direction.

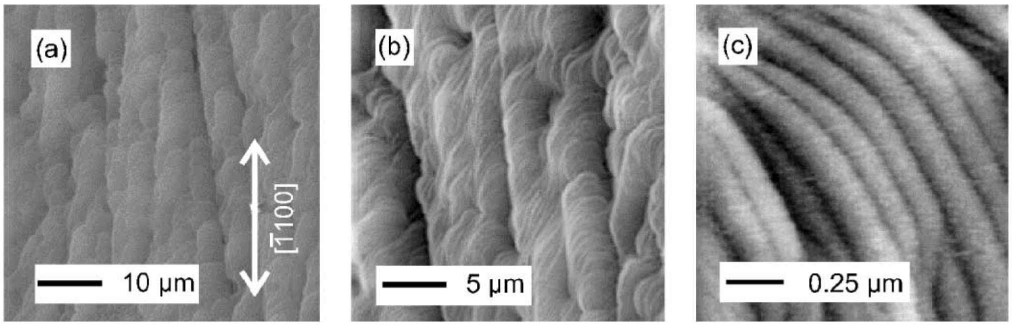

Fig. 4. AFM images obtained on the concave-shaped parts of the SiC after H_2 etching for 1 h at 1700 °C: (a) $50 \times 50\ \mu m^2$ area (vertical range 1 µm); (b) $25 \times 25\ \mu m^2$ area (vertical range 540 nm); (c) $1.4 \times 1.4\ \mu m^2$ area (vertical range 18 nm). This zoom-in reveals that the larger elongated islands are not flat, but are covered by secondary islands with curved step edges.

In Fig. 3(a), the surface is imaged right after grinding with no H_2 etching. A qualitative inspection reveals that the roughness has increased as compared to the flat area of the as-received sample (see inset in Fig. 1) and no indication of a preferential step orientation is seen. Fig. 3(b) shows the sample after H_2 etching for 5 min at 1600 °C and a qualitative analysis reveals the surface morphology has changed. A predominant average

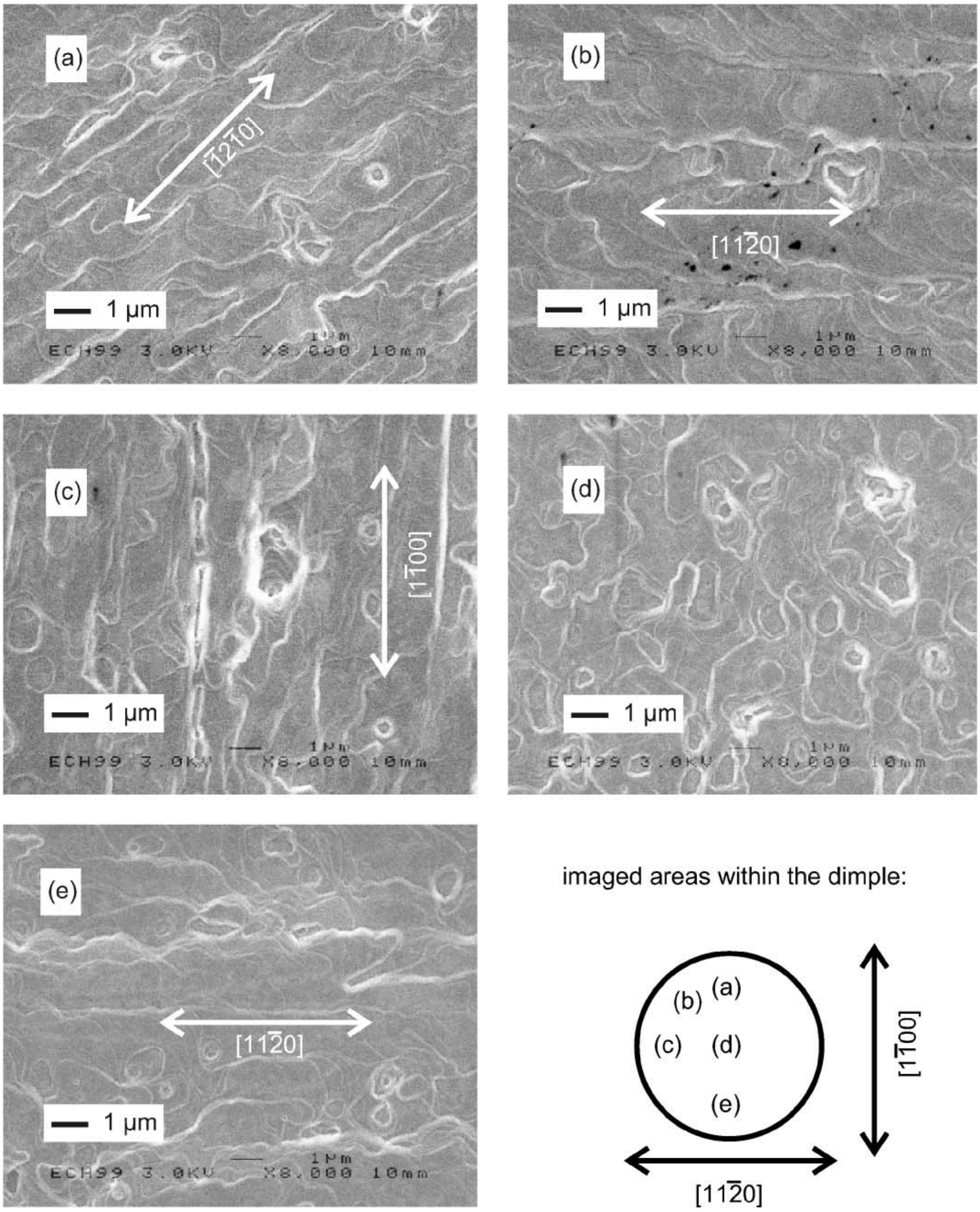

Fig. 5. SEM images taken at different parts in the concave-shaped surface after H_2 etching at 1700 °C for 1 h. A schematic area of the measured locations is given by the sketch. Different locations are characterised by different local misorientations, which give rise to different preferential step edge orientations. See text for details.

island size of the order of 0.5 μm is observed. Individual steps and little terraces are visible, however, mostly as closed steps in rough islands. After additional etching of 15 min at 1600 °C, a slight reorganisation of the morphology resulting in a preferential step orientation along $\{\bar{1}2\bar{1}0\}$ is shown in Fig. 3(c). Isolated islands, separated by deep trenches, which we ascribe to the remainders of scratches produced by the grinding are seen. This ordering of the surface morphology gets more pronounced after etching the sample for an additional 15 min at a more elevated temperature of 1700 °C. The corresponding AFM image is given in Fig. 3(d). A preferential alignment of the island step edges along the $\{\bar{1}2\bar{1}0\}$-direction has evolved but the observed structural features are still rough and irregularly shaped. The overall morphology shows mainly step bunches and the rough islands of Fig. 3(c) have vanished indicating an effective healing of the defects caused by the grinding. The formation of extended terraces is observed only after etching at 1700 °C for 1 h, as discussed below.

The series of AFM images in Fig. 4 gives a zoom into one region in the concave-shaped dimple after this high-temperature etch. Directionally aligned morphological features as presented in Fig. 4(a) show the flattening of the terraces during the etching procedure. The zoom-in of Fig. 4(b) and (c) reveals that the flattening process is not finished at this point. Secondary terraces with a width of the order of 140 nm, on top of the larger size aligned terraces, are found at this etching state, as shown in Fig. 4(c). We suspect that longer H_2 etching might flatten the top islands, thus producing flat terraces even in the concave-shaped regions. These additional experiments have not been performed yet.

So far, only reorganisations observed in one individual region of the dimple have been discussed. The observed preferential alignment of terrace steps along certain crystallographic directions is expected to depend on the azimuthal position within the concave-shaped dimple, reflecting the sixfold symmetry of the SiC crystal. Thus, the effect of both polar and azimuthal misorientation on the H_2 induced morphological changes can be investigated in the dimple.

To study this orientation dependence, we have performed SEM studies of one dimpled sample, which has been etched in H_2 for 15 min at 1700 °C. The regions where the images were taken are indicated by the sketch in Fig. 5. In the centre of the dimple, the local misorientation normal to the surface is nominally zero. There, Fig. 5(d) shows rough hexagonal-shaped islands, which reflect the sixfold symmetry of the SiC. Etching results in the predominance of the most stable step edges, which run along the family of [1 1 −2 0] directions. SEM images taken in the regions (a)–(e) show systematic morphological changes depending on the azimuthal misorientation in the dimple. In Fig. 5(a) and (c), the local miscut, i.e. the average step direction, lies along one of the closed-packed step directions. This allows the energetically stable formation of long and straight step edges, as can be seen in the images. In areas where the average step direction is not along a closed-packed step, as shown in Fig. 5(b) and (e), the formation of long and straight steps is much reduced. Here, kinks are found along the step edges. This can be explained by the fact that straight steps along the local miscut direction are energetically not the most stable steps. Entropy drives the steps to meander between stable, closed-packed orientations which are under an angle to the average step direction causing rough step bunches instead of straight ones.

4. Summary and outlook

First, investigations of the reorganisation of a concave-shaped SiC substrate under H_2 etching are presented. H_2 etching leads to the formation of surface areas with islands with steps aligned in preferential crystallographic directions, as observed by SEM, AFM and STM. The preferential step orientation is ascribed to the atomic structure of closed-packed step edges. Local step structures and alignments reflect the sixfold crystal symmetry. The still rather irregular shape of island and terraces after H_2 etching as compared to the regular morphology observed for Si after thermal treatment [6], reflects the higher thermal stability of SiC. We suggest that the SiC morphology which we present here is largely caused by the kinetics of etching and surface diffusion. Further experiments at higher temperatures are planned to study morphologies which resemble to a better approximation equilibrium structures.

Acknowledgements

Technical assistance of Alain Ranguis and Serge Nitsche, CRMC2, Marseille, are gratefully acknowledged. Two of the authors (W.W. and D.S.) acknowledge the friendly hospitality and support of the CRMC2 and the Université d'Aix Marseille 2.

References

[1] W.J. Choyke, H. Matsunami, G. Pansl (Eds.), Silicon Carbide, Akademie Verlag, Berlin, 1997.

[2] Q. Xue, Q.K. Xue, Y. Hasegawa, I.S.T. Tsong, T. Sakurai, Appl. Phys. Lett. 74 (1999) 2468.

[3] K. Heinz, U. Starke, J. Bernhardt, J. Schardt, Appl. Surf. Sci. 162–163 (2000) 9.

[4] T. Ueda, H. Nishino, H. Matsunami, J. Cryst. Growth 104 (1990) 695.

[5] S. Tanaka, R.S. Kern, R.F. Davis, J.F. Wendelken, J. Xu, Surf. Sci. 350 (1996) 247.

[6] M. Hanbücken, B. Röttger, R. Kliese, I. Vianey, H. Neddermeyer, Europhys. Lett. 23 (1993) 573.

[7] F. Owman, C. Hallin, P. Martensson, E. Janzén, J. Cryst. Growth 167 (1996) 391.

[8] N. Ohtani, M. Katsuno, T. Aigo, T. Fujimoto, H. Tsuge, H. Yashiro, M. Kanaya, J. Cryst. Growth 210 (2000) 613.

[9] C. Hallin, F. Owman, P. Martensson, A. Ellison, A. Konstantinov, O. Kordina, E. Janzén, J. Cryst. Growth 181 (1997) 241.

[10] Z.Y. Xie, C.H. Wei, L.Y. Li, Q.M. Yu, J.H. Edgar, J. Cryst. Growth 217 (2000) 115.

[11] A. Leycuras, Mater. Sci. Forum 338–342 (2000) 241.

[12] VEECO Microscopy Group, Park Scientific Instruments. http://www.tmmicro.com.

[13] OMICRON Vakuumphysik GmbH, Idsteiner Str. 7, D-65232 Taunusstein. http://www.omicron.de.

[14] V. Ramachandran, M.F. Brady, A.R. Smith, R.M. Feenstra, D.W. Greve, J. Electron. Mater. 27 (1998) 308.

[15] R.J. Pechman, X.-S. Wang, J.H. Weaver, Phys. Rev. B 52 (1995) 11412.

[16] R. Madar, M. Anikin, K. Chourou, M. Labeau, M. Pons, E. Blanquet, J.M. Dedulle, C. Bernard, S. Milita, J. Baruchel, Diam. Rel. Mater. 6 (1997) 1249.